Structure and Mass Flux Distribution of a Side-opened Hollow Cone Spray Generated by Swirl Pressure Atomizers

E. Abo-Serie[1*], S. Moon[2] and C. Bae [2]

1 Coventry University, Automotive Engineering Applied Research Group, UK.
2 Korea Advanced Institute of Science and Technology, South Korea

Abstract
A sufficient large taper angle nozzle fitted with a swirl injector proved to provide a robust side-opened spray of which structure is less influenced by the change in the surrounding air pressure and temperature. Nevertheless, the mass distribution of the injected mass is not uniform and it has a distribution that depends on the taper angle and the flow angle. Analysis has been performed to calculate the mass distribution which is a necessary initial condition for spray modeling. The side-opened angle was evaluated for different nozzle taper angles. The derived equation of mass distribution requires previous knowledge of nozzle exit film thickness and flow angle, which were measured experimentally.

Introduction

Direct injection spark ignition (DISI) engine is one of the promising technologies to meet the stringent future engine-out emissions regulations. The low carbon dioxide and fuel consumption especially during the low load conditions is the main advantage of DISI engine. During operation at low and medium loads and speeds, a region of combustible mixture is formed close to the spark plug such that fraction of air inside the combustion chamber is contributing in the combustion process. The combustible region is achieved by injecting the fuel late during the compression stroke shortly before ignition to form a mixture cloud at the spark plug. A key component for realizing stable, lean operation in a DISI engine is the stable repeatable fuel spray. The spray has to be repeatable to achieve a stable fuel vapour cloud around the spark plug has, regardless of the engine speed and load in addition.

The swirl injector was successful in the first-generation of DISI engines using a wall guided combustion system that was implemented in Mitsubushi engine 1996 [1]. This system was depending on the piston cavity to direct the spray and fuel cloud towards the spark plug. However, the spray impingement on the piston wall results in high unburned hydrocarbon (UBHC) emissions due to incomplete mixing and particle formation due to wall wetting.

Different other injectors have been employed for the close the spacing combustion system to provide more robust spray at different engine conditions to avoid engine misfire and torque fluctuations. The spray from a multi-hole injector showed a very small variation in spray structure from one injection and very small variation in spray angle for different engine conditions. However, the multi-hole injector has high penetration at lower back pressure Moreover it has a poor momentum exchange with air which leads to local high fuel concentration at the centreline with sharp gradient [2]. In addition, the injection pressure is higher, 200 bar, in comparison with the swirl injector. The outward-opening piezo-injector which has a hollow cone spray structure with a spray angle mainly controlled by the geometry has then been recently introduced. The spray from such injector provides very well spatial distribution of droplets and therefore better mixing, however, it needs again higher injection pressure to achieve fine spray droplets [2]. Introducing a piezo-cell enables relatively very short injection duration by minimizing the opening and closing times of the needle, however, the high cost is a main concern of DISI engine manufacturer

Swirl injectors have the advantage of producing well-atomized spray at lower injection pressure compared to non-swirling sprays. However, previous studies showed that swirling spray is sensitive to air flow condition that cause significant change in its geometry and the microscopic structure; droplet size and velocity distribution [3]. Changing fuel temperature can also cause significant variation in the spray geometry and structure [4]. This change in spray characteristics make it inappropriate for gasoline direct injection engine that uses spray guided combustion system, which as mentioned earlier, requires more repeatable robust spray under different engine operating conditions to avoid engine misfire.

The variation in swirling spray characteristics could mainly be attributed to the complex air structure formed in the inner part of the spray envelope. Having momentum exchange from the swirling liquid to the air will lead to the formation of a forced vortex air swirling flow in the inner part of the spray. This vortex could have a swirl number larger than the critical value that can lead to a counter flow vortex which naturally pressing causing pressure drop and fluctuations acting on the inner side of the spray envelop [5]. This complex nature of the air flow varies with engine air flow conditions; pressure and temperature and leads to different spray geometry. For the swirl injector to be

Dr. E. Abo-Serie: e.abo-serie@coventry.ac.uk
www.coventry.ac.uk
Proceedings of the 21th ILASS-Europe Meeting 2007

used in DISI engine with spray guided system, the nozzle has to be modified such that the air pressure inside the spray-envelop can be balanced with that at its outer side. This can be achieved by a taper nozzle with specific taper angle [6]. Having a swirl injector with a taper nozzle could deliver a robust spray that does not vary with engine operating conditions and ca potentially used in DISI engines.

This study pays more attention to the spatial mass distribution from this injector. It provides a mathematical analysis and a final equation that can calculate the mass distribution at the nozzle exit based on previous given information about the liquid film thickness and the flow angle at the nozzle exit.

Experimental Work

a taper nozzle was manufactured with a taper angle 70 degree and attached to the main nozzle as shown in Figure 1.

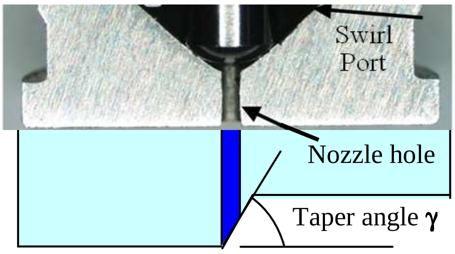

Figure 1 Schematic of the taper nozzle attached to the main nozzle of a DISI swirl injector

The spray was visualized under atmospheric conditions in a wind tunnel and at different back pressure in a constant volume chamber. A CCD camera with a resolution of 1280x1024 pixels (Sencicam) was used to visualize the spray at different times from the start of injection signal. The injector was driven using a timed card that also provides a triggering signal to the camera. A laser sheet formed by a 6 W Argon-Ion laser (Spectra Physics) was used a light source. The conditions used during the experiments are shown in Table 1.

Taper angle	70o
Injection pressure	5MPa, 7MPa
Fuel temperature	298K, 358K, 393K
Ambient pressure	0.1MPa, 0.5MPa, 1MPa
Ambient temperature	Atmospheric
Fuel	Commercial gasoline

Table 1 Operating conditions for spray images

To measure the fuel droplet size distribution, a phase Doppler anemometry (PDA) was utilized with a transparent steady flow rig as shown in Fig. 1. The dimension of the wind tunnel transparent cross section is 200 mm by 200 mm. The setup parameters of the PDA system are optimized to enables measuring maximum diameter of 60 mm and velocities between -7.5 m/s to 56 m/s. The spray droplets at all the measurement points were collected during 500 injections.

For the purpose of measuring the film thickness inside the nozzle, a transparent nozzle was attached to the main nozzle and back lighting technique was used [4].

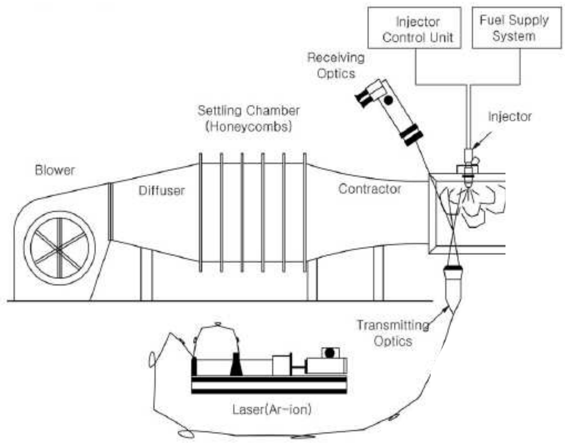

Figure 2. Schematic of the PDA arrangement for droplet velocity and size measurements

Results and Discussions

<u>Spray images and PDA results</u>

To have a side-opened spray, the taper angle of the nozzle has to be larger the complement of the flow angle. This allows the stream lines of the liquid film formed inside the nozzle to flow parallel or away from the nozzle exit edge from one side of the nozzle without exiting the nozzle while exits the nozzle from the other side.

The spray images of a 70 degree taper angle nozzle and a flow angle of 30 degree at different times for different back pressures show that the structure of the spray is very similar, as shown in Fig 3. The penetration of the spray as expected decreases with increasing the chamber air pressure as a result of the higher drag associated with higher air density. However the spray angle variation is very small compare to the case with the typical nozzle of the swirl injector as shown in Figure 4. Having a wide side-open area in the spray envelope allows the pressure of the air located inside the spray envelope to be balanced with the chamber air pressure and thus, eliminates the local pressure variation that leads to the complex air flow structure inside the spray envelop [5]. The spray structure becomes similar to a fan spray generated by slit injectors [7]. However the advantage of using the swirl injector is the lower injection pressure and spray penetration without scarifying the quality of atomization.

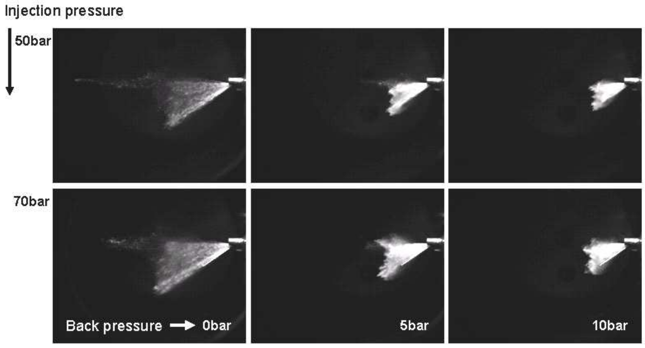

Figure 3 Spray images of a 70 degree tapered nozzle at different injection and air back pressures.

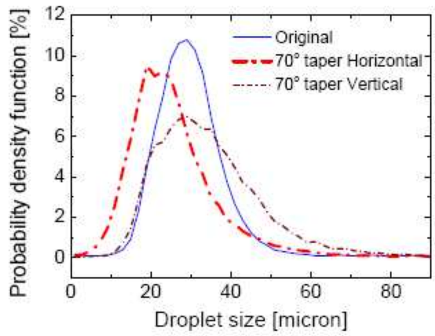

Figure 6 Comparison between droplet size distribution of a taper nozzle and a traditional swirl nozzle.

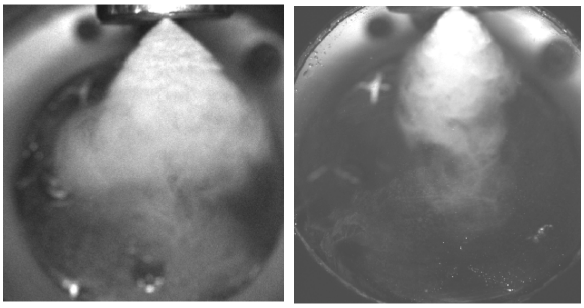

Figure 4 Spray images of a typical swirl nozzle at different injection and back pressure.

Droplet diameter distribution obtained at a horizontal section (see Figure 6) showed smaller diameter and lower sauter mean diameter as shown in Figure 5. This could be attributed to the larger area where the spray exiting the nozzle and thus there is less possibility of coalescence. It was also noticed that the spray angle is larger than that from a typical swirl nozzle. At the edge of the spray (vertical locations), the droplet sizes were noticeably large. The large droplets located at the edge of the spray were also observed at the edge of fan type sprays produced by slit injectors in different studies. It was attributed to thickening of the edge of the liquid film as a result of surface tension before it is atomized [7].

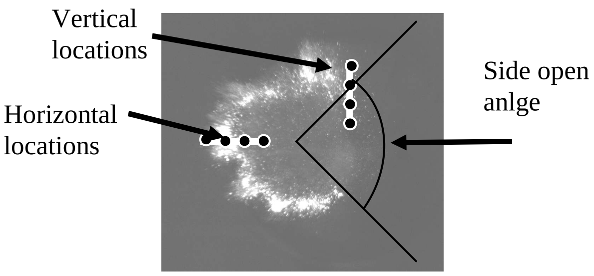

Figure 5 Locations of droplet size measurements

<u>Nozzle mass distribution calculations</u>

To calculate the mass flow rate, the velocity components along the peripheral of the nozzle exit have to be known. In this study, the velocity at the nozzle exit was identified by visualizing the liquid film inside a transparent nozzle attached to the main nozzle. Images were processed to identify the average liquid film thickness of 50 images, see figure 7a. The average injection mass flow rate and film thickness were then used to calculate the average axial velocity by applying the mass conservation equation. Instead of measuring the film thickness, a two phase model using VOF method has proved to provide a good estimate to the film thickness if the swirler and nozzle geometries are known [8]. The swirling motion of the liquid at the nozzle exit was identified by imaging the surface of the liquid very close to the nozzle exit with relatively longer exposure time. This method allows to capture the streams of the pathway of the liquid and therefore the flow angle (α), as shown in Figure 7b.

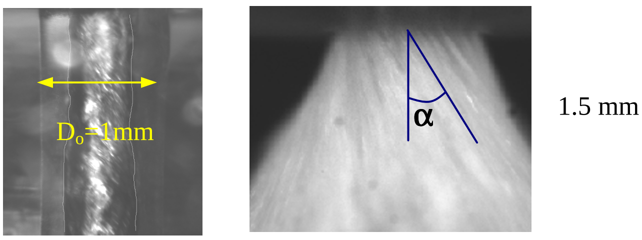

(a) film thickness (b) flow angle

Figure 7 Images showing the flow inside a transparent nozzle and near the nozzle exit

To identify the mass exiting the taper nozzle, the velocity perpendicular to the nozzle exit plane has to be calculated for different angle θ, as shown in figure 8. Assuming the axial and tangential velocities at the nozzle exit are constant, their values can be calculated as follows:

$$U_a = - U_z \text{, and } U_t = U_a \tan \alpha \qquad (1)$$

where, α is the flow angle that has been measured from the images. From the geometry, the velocity normal to the nozzle exit plane, U_N, can be calculated as follows:

$$U_N = - U_t \sin\theta \sin\gamma - U_a \cos\gamma \qquad (2)$$

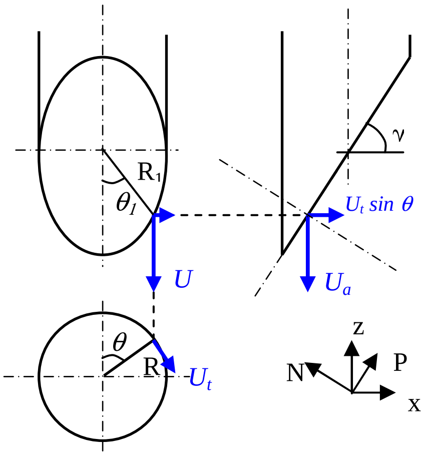

Figure 8 Schematic showing the taper nozzle in the three planes and the liquid film velocities.

The mass flow rate of the liquid through an angle dθ can be calculated as follows:

$$dm^{\cdot} = \rho U_N h \ \ ds \qquad (3)$$

where h is the film thickness, ρ is the liquid density and ds is the arc length correspond to a an angle dθ.

An approximate estimate of the arc length ds corresponding to an angle dθ could be deduced from the following equation:

$$ds = \sqrt{{R_2}^2 + \left(\frac{dR_2}{d\theta}\right)^2} \ d\theta \qquad (4)$$

where R2 is the radius of the ellipse on the face of the taper nozzle at any angle θ . Notice that R2 is different than R1 shown in the Figure 8 This radius could be derived from the geometry and have the form:

$${R_2}^2 = \frac{R^2 \cos^2\theta}{\cos^2\gamma} + R^2 \sin^2\theta \qquad (5)$$

Equation 4 and 5 can be used to derive equation 6 for the arc length at different angle θ within an angle variation dθ a. Finally, equation 7 representing the mass distribution at the nozzle exit can be derived by substituting equations 1,2 and 6 into equation 3.

The mass distributions for different taper angles and flow angle of 30 degree are shown in Figure 9. This figure shows a significant difference between the mass exiting the nozzle from one side compare to that from the other side. Clearly as the taper angle increases, the quantity of liquid fuel exiting from one side decreases until it reaches a critical value where no mass exiting the nozzle, at a specific location which is correspond to an angle (θ) -90 degree. This is location where the spray will start to open. At this critical taper angle and -90 degree, the liquid inside the nozzle moves parallel to the nozzle cut edge without exiting the nozzle. This critical taper angle is the complement of the flow angle. At the opposite side of the nozzle at an angle +90 degree the amount of mass decreases with the taper angle.

To further explain the variation of the mass distribution at the nozzle exit, the velocity normal to the exiting plane of the nozzle is plotted for different taper angles, in Figure 10. This figure shows the angle at which the velocity becomes negative and therefore, the location where there is no mass exiting the nozzle. It shows also that increasing the taper angle leads to a reduction in the flow velocity normal to the exiting plane. Nevertheless, the exiting area of the liquid becomes larger due to the increase in the radius and thus the arc length corresponding to one degree angle, as shown in Figure 11. For an angle 90 and -90, the area is not changing since the radius is the same for any taper angle and thus the corresponding arc length remains constant.

To have a stable and robust spray the opening angle has to be sufficiently large to allow a quick balance for the pressure between the air located inside and outside the spray envelop. It is, therefore, important to estimate this side-opened angle for different taper angles. This relationship could be deduced by solving equation 7 considering the mass flow rate is equal to zero. Solving this equation will lead to equation 9 which identify the angle at which the mass flow rate reaches the zero value. Accordingly, the relationship between the flow angle and the taper angle for different open side angle can be established as equation 10. Baring in mind, equation 9 is only valid for a taper angle larger than the complement of the flow angle:

$$ds = R\sqrt{\frac{\cos^2\theta}{\cos^2\gamma} + \frac{4\cos^2\theta\ \sin^2\theta\ (\cos^2\gamma - 1)^2}{\cos^2\gamma\ (\cos^2\theta + \sin^2\theta\ \cos^2\gamma)} + \sin^2\theta} \ \ d\theta \qquad (6)$$

And the volume of mass injected at an angle θ within a step of $d\theta$ becomes:

$$dm = \rho\ R\ h\ (U_a \tan\alpha\ \sin\theta\ \sin\gamma + U_a \cos\gamma)\sqrt{\frac{\cos^2\theta}{\cos^2\gamma} + \frac{4\cos^2\theta\ \sin^2\theta\ (\cos^2\gamma - 1)^2}{\cos^2\gamma\ (\cos^2\theta + \sin^2\theta\ \cos^2\gamma)} + \sin^2\theta} \ \ d\theta \qquad (7)$$

$$\sin\theta = \frac{-1}{\tan\alpha \ \tan\gamma} \qquad (9)$$

where, $\gamma \geq (90-\alpha)$

$$\text{Sid-opened angle} = 2(90-\theta) \qquad (10)$$

The actual angle could be larger than the value calculated here, due to the thickening of the edge of the liquid film after exiting the nozzle and before being atomized, as observed in other studies using fan sprays [7]. The variation of the side-opened angle for different taper angles is shown in Figure 12

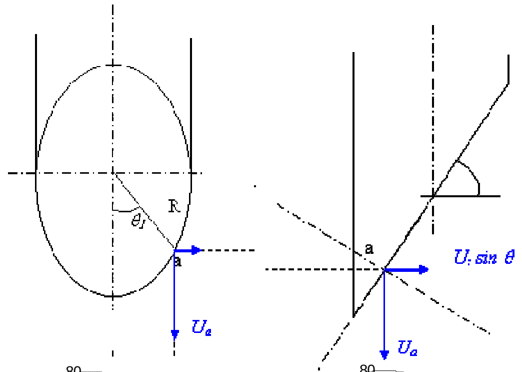

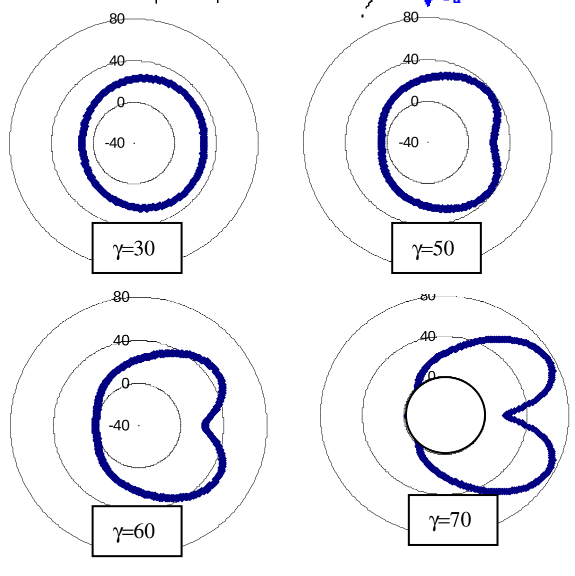

Figure 9 The distribution of liquid injected volume for different taper angles.

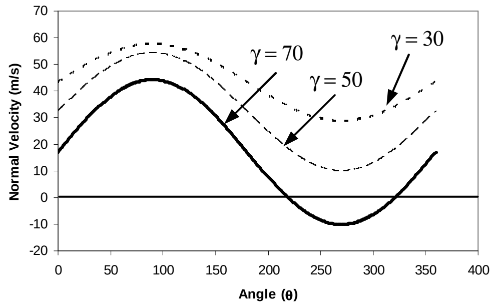

Figure 10 Normal velocity variations for different tape angles for a flow angle of 30 degree

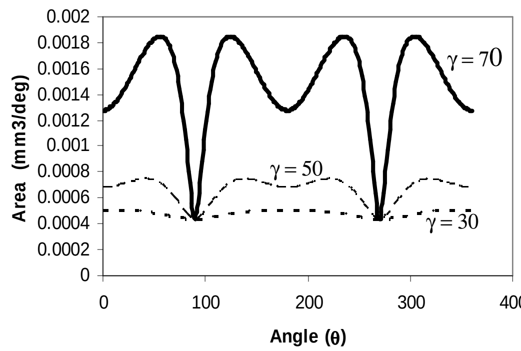

Figure 11 The exiting area distribution for different taper angle for a flow angle of 30 degree

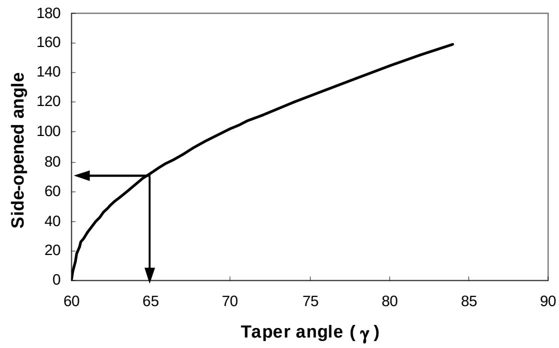

Figure 12 Variation of open side angle of the spray for different taper angle (γ) for a flow angle of 30 degree

Increasing the taper angle by 5 degree more the complement of the flow angle causing the spray to have a side opened angle of 72 degree. More increase in the taper angle leads to approximately linear increase in the side opened angel as shown in Figure 12.

Spray mass distribution

The mass distribution of the liquid fuel is very crucial in the mixing process and therefore combustion stability and engine out emissions. It is worth mentioning that spray liquid distribution is not only affected by the nozzle initial distribution but also by the aerodynamic force from the air flow. To achieve the required air/liquid distribution, the initial nozzle distribution has to be optimized with the air flow pattern.

Although machining the nozzle to form a taper exit shape provides larger exit area in comparison with normal nozzle (zero taper angle), the utilized area for the liquid to exit the nozzle could be smaller depending on the side-opened angle. Previous section demonstrated that the utilized area not only could be smaller but also within the area where the fuel exiting the nozzle, the mass is not uniformly distributed. This initial injected distribution of mass exiting the nozzle leads to uneven spatial distribution of liquid within the main stream of the liquid spray. Further downstream of the injector, this distribution is altered due to the tangential velocity acquired from the liquid film swirl motion. This alteration is not simply rotation of the injected mass distribution as the spray penetrates downstream due to the variation in aerodynamic forces with droplet sizes. The large droplets have larger momentum and can survive longer while the smaller droplets lose their momentum quickly and follow the air motion. Air entrainment and air flow pattern around the spray plays another main role in redistribution the droplets within the liquid spray, especially when the droplets lose their own momentums. The location of smaller droplets and the larger droplets are usually other concern for mixing process.

Modeling the spray could provide valuable information that can assist in optimizing the airflow to re-arrange the droplet to achieve an optimum spatial distribution of spray droplets within the combustion chamber.

Conclusions

A swirling spray with a side-open in its envelop using a taper nozzle was proved to be more robust and less sensitive to air surrounding conditions than the traditional hollow cone spray. To form a side-opened spray, the taper angle has to be larger than the complement of the flow angle at the nozzle exit. Analysis has been presented to calculate the mass distribution and the side-opened angle for different nozzle taper angles. The work presented here also shows there is a potential to have different nozzle shapes but special attention has to be paid to the mass distribution at the nozzle exit.

References

1. Y. Iwamoto, K. Noma, O. Nakayama, T. Yamauchi, H. Ando, Development of Direct Injection Gasoline Engine, SAE970541, 1997

2. M. Skogsberg, P. Dahlander and I. Denbratt, Spray Shape and Atomization Quality of an Outward-Opening Piezo Gasoline DI Injector, SAE 2007-01-1409, 2007

3- Abo-Serie E., Arcoumanis C., Gavaises, M. ,Spray characteristics of swirl pressure atomizers for G-DI engines: Phase Doppler measurements, ILASS-Europe, 11-13 September, 2000, Darmstadt, Germany

4- Moon, S., Bae, C., Abo-Serie, E. and Choi, J., Internal and near nozzle flow of a pressure-swirl atomizer under varied fuel temperature, Atomization and Sprays, Vol. 17, 2007

5- Syred, N. ,A review of oscillation mechanisms and the role of precessing vortex core (PVC) in swirl combustion systems, Progress in Energy and Combustion Science, Vol. 32. PP 93-161, 2006.

6- Moon, S., Yoon, H., Abo-Serie, E. and Bae, C. ,Generation of Robust and Well-Atomized Swirl Spray, JSAE 20077258 /SAE 2007-01-1852, 2007

7- Atsuya Okamoto, Takaaki Sato and Naotaka Shirabe, Yukinobu Anezaki, Development of Fan Spray Simulation for Gasoline Direct Injection Engines, SAE 2001-01-0962, 2001

8- Gavaises, M. and Arcoumanis, C., Modelling of Sprays From High-pressure Swirl Atomizers, Int. J. Engine Research. Vol. 2, No. 2, 2001